Biosensors and Bioelectronics 128 (2019) 9–16

Contents lists available at ScienceDirect

Biosensors and Bioelectronics

journal homepage: www.elsevier.com/locate/bios

Paper-based miniaturized immunosensor for naked eye ALP detection based on digital image colorimetry integrated with smartphone

Kuldeep Mahato, Pranjal Chandra*

Laboratory of Bio-Physio Sensors and Nanobioengineering, Department of Bioscience and Bioengineering, Indian Institute of Technology Guwahati, Assam 781039, India

ARTICLE INFO

Keywords:
Paper biosensor
Alkaline phosphatase
Bioanalysis
Digital image colorimetry, Miniaturized prototype

ABSTRACT

Alkaline phosphatase (ALP) is a metalloprotein found naturally in raw milk samples and is considered as an important biomarker in quality control of milk. Its easy, personalized, as well as instrument-less detection is important to ensure the pasteurization and its differentiation form raw milk. In view of such importance of APL, we have developed an office punching machine crafted paper biosensor for naked eye detection of ALP in milk samples. The quantitative estimation is done by digital image colorimetry (DIC) based technique integrated with smartphone. The sensor-probe was developed by the covalent immobilization of ALP antibody (anti-ALP) onto the functionalized paper surface. The fabrication of the biosensing probe was characterized using DIC, Fourier transform infrared spectroscopy (FTIR), and atomic force microscopy (AFM). The detection was based on immunocomplexation between the sensor-probe and ALP, which generates blue-green precipitate as an analytical signal by exploiting the catalytic activity of ALP towards 5-bromo-4-chloro 3-indolyl phosphate (BCIP). The dose dependent appearance of the blue-green complex was captured using smartphone camera and DIC was employed using Red, Green, and Blue (RGB) profiling system, where the maximum sensitivity was obtained for the red color channel. Based on the DIC analysis, a wide dynamic range for the ALP detection is obtained from 10 to 1000 U/mL with the detection limit of 0.87 (± 0.07) U/mL. The designed paper-based biosensor is successfully applied to detect ALP in commercial and raw milk samples. Interferences due to components present in the milk samples was evaluated and the long-term stability of the designed biosensor was examined. Based on the detection principle, a miniaturized kit [20.0 mm (*L*) × 20.0 mm (*W*) × 2.15 mm (*H*)] was developed and applied for the ALP detection to demonstrate the instrument-free direct in-kitchen applicability.

1. Introduction

Milk has been a part of various traditional and contemporary servings across the globe, which not only enriched with high amount of proteins, carbohydrates, and fats; but also contains vitamins as well as different essential minerals (Gaucheron, 2011). Due to its immensely high nutritional impact on mankind, milk has been accepted as noble and stable food worldwide. In addition to this, milk contributes exceptionally high amounts of the calcium dietary reference intake (52–65%) (Rozenberg et al., 2016). The milk quality and its freshness have been a major concern, as the post-milking invasion of microbes causes sourness and are capable of harboring pathogenic bacteria, which not only downgrades the taste and quality of the milk, but also adds high chances of food borne disease if consumed (Jay-Russell, 2010). In industries, raw milk is processed through pasteurization to kill the pathogenic microbes, which is an important step to maintain/extend the shelf life of milk. To ensure the effective pasteurization, several methods, including methylene blue, phenol-based tests (Fasken and McClure, 1940), and microbial culturing are commonly used in the quality control centers of various industries (Nayak, 2018; Yalcin and Atasever, 2018). In methylene blue (MB) based tests, the dye is used as the redox indicator, which is injected into the milk samples followed by heat treatment and kept until the appearance of color change and therefore it takes 30–480 min for the assessment depending on the milk samples (Barkworth and Hosking, 1952). Due to its time-consuming process, it is not always preferred in the quality controls, especially where the number of samples are very large. Additionally, the commercial phenol-based tests utilizes the modified Scharer's colorimetric method, where liberated phenol is measured with the help of an indicator 2,6-dibromoquinonechloroimide (Payne and Wilbey, 2009; Scharer, 1938). These tests require sophisticated spectrophotometers and involves multistep procedure, which restricts them for onsite detection. Tests based on the microbial culture requires special laboratory facility and usually take longer time for analysis. Limitations associated

* Corresponding author.
E-mail address: pchandra13@iitg.ac.in (P. Chandra).

https://doi.org/10.1016/j.bios.2018.12.006

Available online 18 December 2018

with these conventional testing procedures make them non-robust and unsuitable for the assessment in miniaturized settings for determination at the point of collection, which is foremost need to ensure the quality of milk. Therefore, it is important and would be interesting to attempt a new biomarker-based method to differentiate the pasteurized and raw milk utilizing advanced bioengineering approaches.

Among various indicators of pasteurization and good quality milk, ALP, a metalloenzyme is widely targeted because of its heat resistant property, which has close destruction point to the killing temperature of pathogenic microbes (Rankin et al., 2010; Soares et al., 2013). Moreover, considerably high concentrations of ALP is found in raw milk, which denatures after the pasteurization process (Rankin et al., 2010), hence in an ideal situation the pasteurized milk should be devoid of ALP. Additionally, it has also been reported that in case of mastitis the ALP concentration in milk is tremendously high (Babaei et al., 2007; Kitchen, 1981). Therefore, processing of such milk in industry requires special attention, and to do so, the detection of ALP in raw and pasteurized milk has tremendous commercial as well as health interest. In view of such importance of ALP in milk, several attempts have been taken to detect the ALP by various approaches; including spectroscopic (Al-Qadiri et al., 2008), fluorimetric (Kulmyrzaev et al., 2005; Rola and Sosnowski, 2010), electrochemical (Ito et al., 2000; Serra et al., 2005), electro-chemi-luminescence (Park et al., 2011), and ELISA (Chen et al., 2006). Despite of their recognizable detection performance in native milk; multistep nature, requirement of sophisticated bulky analytical instruments as well as trained personnel, limit their usage in remote settings and in home kitchens. Therefore, development of a new user-friendly and economical method for ALP detection is of great interest. In order to develop such miniaturize devices, various research and development activities have been performed in recent past to introduce a portable testing kits (Chandan et al., 2015).

Among all types of testing kits, paper-based detection systems have found commercial interest because of their low-cost, adequate availability, and environment-friendly nature (Mahato et al., 2017). A paper-based approach has rarely been attempted for the detection of ALP in milk samples. In one such approach, ALP has been detected based on a colorimetric lateral flow assay (LFA) (Yu et al., 2015), which sometime suffers due to the irregularities in porosity causing interruption in flow of target molecule in the paper matrix due to the clogging of pores (Hosseini et al., 2017). This method based on LFA relies on the indirect ALP detection using adsorbed antibodies in the sensing matrix (Yu et al., 2015). The adsorbed antibodies in a sensing matrix are not homogeneously oriented compared to antibodies those are immobilized on to the surface using various conjugation methods (Tajima et al., 2011; Trilling et al., 2013). This may eventually compromise the analytical performance of biosensors. Therefore, it is extremely important to have stable and well oriented immobilization of antibodies onto the paper matrix and a dot-spot-based sensor chip. Stable immobilization of antibody retaining its biological activity can be achieved through conventional covalent immobilization processes (Akhtar et al., 2018; Chandra et al., 2012). Apart from this, the paper-based onsite colorimetric detections are mostly qualitative/semi-quantitative in nature (Yetisen et al., 2013), therefore several attempts have been given to quantify the “yes/no” signals, but the usage of additional analyzer confines the applicability of these in limited resources. Recent paradigm has been shifted toward the elimination of such dedicated analyzers and thus, smartphone being an omnipresent self-sufficient device has recently found the global attention for personalized analyses. A technique based on the image analysis also called DIC have gained attention for quantitative colorimetric estimations, which is one of the rapidly emerging robust technique (Rateni et al., 2017). Fundamentally, the DIC is based on image acquisition and its processing to obtain the quantifiable data-points, where former is performed by digital camera and latter is done with the help of analyzer software or smartphone-based application (Rateni et al., 2017). The images of color changing objects are digitally recorded in terms of the pixels, where 8-bit convention is universally accepted. According to this convention, colored image consists of three primary color channels, where 256 (0–255) unit pixel values are allocated of every primary color for the different shades i.e. RGB (Choodum et al., 2017; Parkin, 2016) vary on the intensity and color change. Using these unit pixel values, one can obtain the calibration plot for almost every colorimetric changes for biomolecular analysis (Lin et al., 2018; Peng et al., 2017).

In view of such developments, here in this present work, we have developed a very simple, onsite, quantitative detection of ALP using DIC-based paper sensor. An office punch crafted filter paper discs were used to fabricate sensing probe for the naked eye detection of ALP. The sensor-probe was fabricated by functionalization of paper discs for the covalent immobilization of Anti-ALP. The step by step characterization of the sensor-probe was evaluated by FTIR and DIC. The analytical signals were obtained based on the reaction between ALP bound sensor-probe and BCIP generating quantifiable blue-green precipitate, which were further processed using smartphone to obtain the quantitative results. Direct detection of ALP in commercial as well as raw milk obtained from the villages were performed using standard addition and spike-recovery methods. The selectivity and shelf-life of the developed biosensor was examined to evaluate its real market potential. Finally, a miniaturized prototype was developed for ALP detection to establish the direct in-kitchen household applicability of the designed biosensor.

2. Experimental

2.1. Materials, apparatus, and reagent preparation

The materials used for the experimentation were purchased from standard companies and all the solutions used were prepared using routine laboratory methods. For the characterization of the sensor-probe fabrication different analytical instruments have been used. Details of the materials, instrument used and the procedures are described in Section SI 1 of supplementary-information.

2.2. Fabrication of biosensor

At first stage, Whatman filter paper (P) grade 1 was chosen as the base material for sensor-probe fabrication. The paper discs were cut using office paper punching machine and were carboxylated using 4-carboxybenzene diazonium (DS) solution for six hours followed by thorough washing with distilled water forming P/DS surface. Thereafter, the washed P/DS discs were treated with freshly prepared EDC/NHS (143–100 mM) to activate the –COOH groups at P/DS surface. This was followed by immobilization of Anti-ALP (1.7 μg/μL), which occurred due to the interaction between the $–NH_2$ groups of Anti-ALP and –COOH groups of functionalized P/DS surface. The final sensing probe after Anti-ALP immobilization was represented as P/DS/EDC-NHS/Anti-ALP probe. In order to minimize the nonspecific interaction of ALP and to avoid false positive signals, the P/DS/EDC-NHS/Anti-ALP probe was treated with 1% BSA for 30 mins. In order to remove the unabsorbed BSA, the sensor-probe was washed using sterile PBS-Tween (1.0%) for 1.0 min followed by gentle rinsing with PBS. The formation of each layers of the developed biosensor was examined by FTIR and DIC. The detailed schematic representation of probe fabrication process and principle involved in signal generation have been shown in Scheme 1

2.3. Detection of ALP using the P/DS/EDC-NHS/Anti-ALP biosensor

The detection of ALP relies on the immunocomplexation reaction between P/DS/EDC-NHS/Anti-ALP probe and ALP. For this purpose, varying concentrations of ALP was treated with the designed sensor-probe and allowed to react for 13.0 min. After this, the immunocomplexed assembly (P/DS/EDC-NHS/Anti-ALP/ALP) was gently washed with PBS and allowed to react with BCIP (10.0 mM), producing

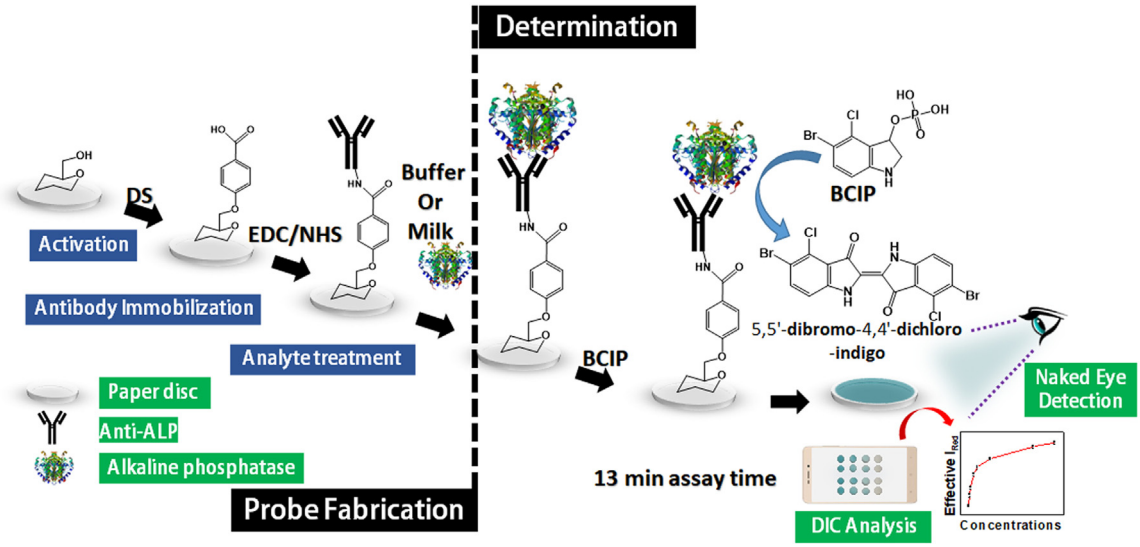

Scheme 1. Schematic representation of the ALP biosensor fabrication and detection principle.

a blue-green colored complex catalyzed by ALP, which was bound to the P/DS/EDC-NHS/Anti-ALP probe surface. A detailed biochemical reaction involving the color generation has been shown is Fig. SI 1 in the supplementary-information section (SI). The color change on paper discs were then recorded by smartphone camera in photographic conditions as mentioned in the Table SI 1. This was followed by the image processing and colorimetric quantification, where the colored images of the paper surface was processed to obtain the corresponding RGB values. To eliminate the errors in pixel values in capturing condition and to avoid the false positive signals of the darker imprints left by the evaporated liquids at the edges of paper substrate, a uniform selective area was adapted for the image analysis. The selective area not only eliminates the dark rings and patches, but also provides the accurate changes in the pixel values by taking mean intensity values of the distributed uniform area. The effective RGB intensities of the colored paper discs were estimated by Eq. (1),

$$Effective\ I_{RGB} = \log_{10}\left(\frac{I_{RGB(Blank)}}{I_{RGB(Conc.)}}\right) \quad (1)$$

where, I_{RGB} is the mean pixel intensities of all primary channels obtained from selected area of BCIP treated P/DS/EDC-NHS/Anti-ALP/ALP discs.

3. Results and discussion

3.1. Selection of color channel for biosensing studies

In order to evaluate the biosensing studies, the RGB convention of image analysis was followed, where we firstly selected the most sensitive primary color channel. In digital images, the I_{RGB} reflects pixel intensity of the true color (blue-green color in our case), which is composed of the intensities of three primary color channels, denoted as I_{Red}, I_{Green}, and I_{Blue}. In the colorimetric changes, gradual intensification of appeared color signifies the absorption of the complimentary color (Firdaus et al., 2014). In order to find out the color channel that provides maximum sensitivity for the analytical applications of the designed biosensor, we individually tested and compared the primary color channels. Fig. 1(A-D) shows the time dependent appearance of the blue-green precipitate on the sensing probe and its corresponding histograms in RGB and R modes at 1.0 (A), 4.0 (B), 8.0 (C), 12.0 (D) minutes. Thereafter, we calculated the time dependent Effective I_{Red}, Effective I_{Green}, and Effective I_{Blue} from 1.0 to 12.0 min separately and plotted the time dependent plot from the obtained data (Fig. 1E). It was interesting to note that the maximum signal was obtained for Effective I_{Red} (0.0094 (± 0.0007) a.u./min), compared to the Effective I_{Green} (0.0019 (± 0.0005) a.u./min) and Effective I_{Blue} (0.0002 (± 0.0011) a.u./min), which was statistically significant ($p < 0.001;\ n=3$). Therefore, in all subsequent biosensing experiments, Effective I_{Red} has been used as an analytical signal which was calculated using Eq. (2).

$$Effective\ I_{Red} = \log_{10}\left(\frac{I_{Red\ (Blank)}}{I_{Red\ (Conc.)}}\right) \quad (2)$$

where, I_{Red} is the mean pixel intensity of red channel obtained from the selected area of BCIP treated P/DS/EDC-NHS/Anti-ALP/ALP discs.

3.2. Characterization of P/DS/EDC-NHS/Anti-ALP biosensing probe

The characterization of the sensing probe was done by DIC and FTIR. At first phase, to confirm the step wise construction of the biosensor, an immunocomplexation experiment was performed. For this purpose, ALP was allowed to react with the P/DS/EDC-NHS/Anti-ALP sensing probe followed by washing and treatment with BCIP, which forms the blue-green precipitates as shown in Fig. 2A **(i)**. In order to confirm that the signal was merely due to the immunocomplexation followed by the catalytic reaction between ALP and BCIP, we characterized the sensing surface by performing series of control experiments. In the first experiment, ALP was allowed to react with the Anti-ALP unimmobilized paper surface followed by its interaction with BCIP (P/DS/ALP/BCIP) **(ii)**. In the second experiment, no BCIP was treated after at the immunocomplexed sensor-probe (P/DS/EDC-NHS/Anti-ALP/ALP) **(iii)**; whereas, in the third control experiment, no ALP was reacted with the sensing probe, but it was treated with BCIP in the final step (P/DS/EDC-NHS/Anti-ALP/BCIP) **(iv).** Interestingly, in all control experiments, no significant Effective I_{Red} was observed ($p < 0.001;\ n = 3$), compared to the Effective I_{Red} which was observed in the case of complete sensing probe i.e. P/DS/EDC-NHS/Anti-ALP/ALP in presence of BCIP. These results clearly indicate that the sensing probe has been correctly developed and is able to detect ALP.

In order to reconfirm the biosensor construction, each layer of the sensor-probe was characterized using FTIR. The representative FTIR spectra for bare paper (P) substrate, diazonium treated paper (P/DS), EDC-NHS activated paper (P/DS/EDC-NHS), and antibody immobilized paper surface (P/DS/EDC-NHS/Anti-ALP) have been shown in Fig. 2B. For the P (i), peaks between 1000 and 1200 cm^{-1}, 2995 cm^{-1}, and 3257 cm^{-1} were observed, which are due to the C-O-C and C-C-C vibrations, C-H stretching, and O-H stretching vibrations, respectively.

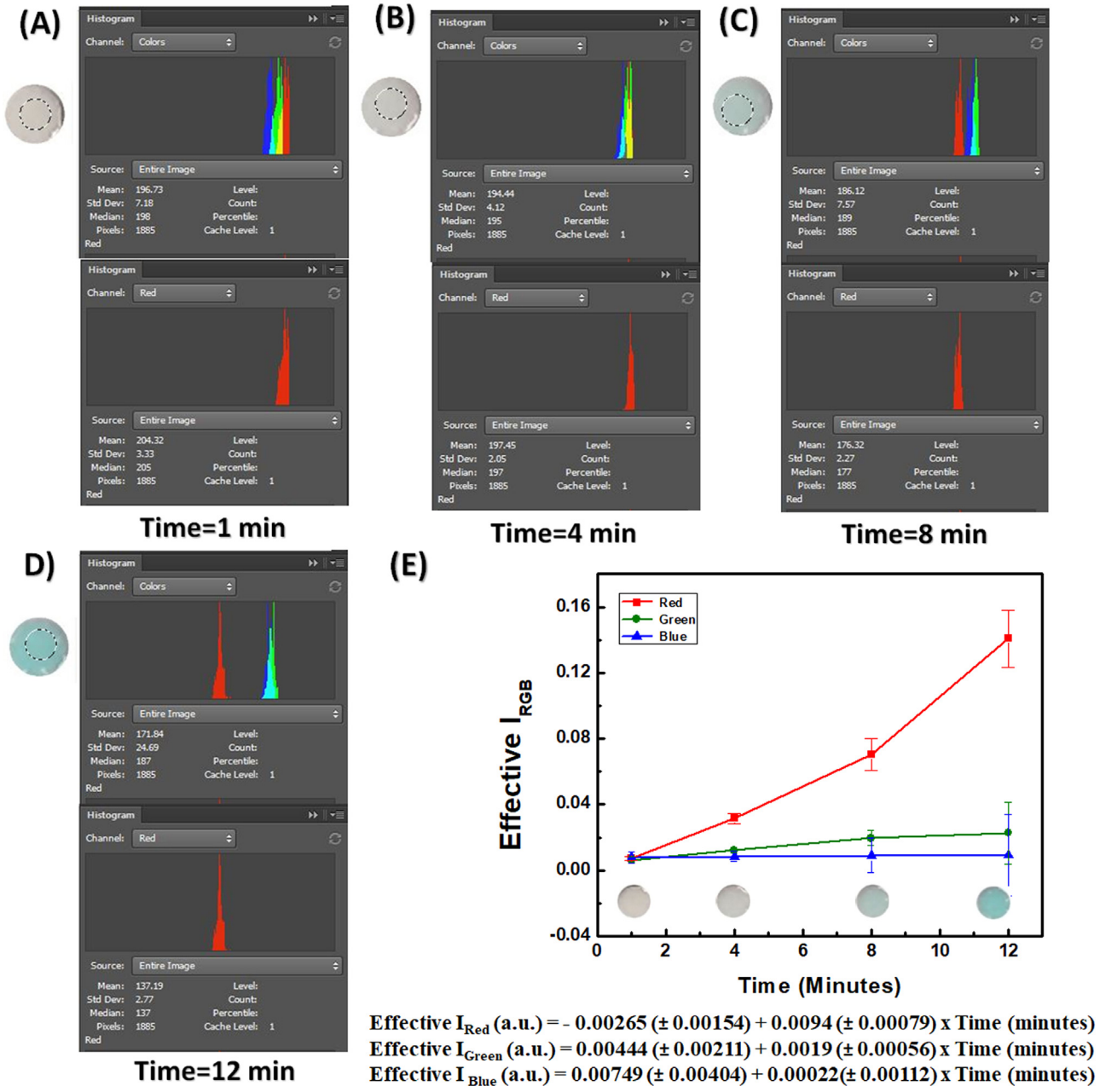

Fig. 1. (A) Histogram showing gradual change of RGB and R intensities with time (i-iv) (using Adobe Photoshop tool) and (v) shows the corresponding plot obtained for Effective I_{Red}, I_{Green}, and I_{Blue}.

After the treatment with diazonium solution, (ii) the appearance of peak at 1700 cm^{-1} and 1515 cm^{-1} correspond to the carboxyl group (C=O) and aryl (C=C), respectively; which are most likely due to the addition of caboxybenzyl flanking groups on to the cellulose fiber of the paper forming (P/DS). After the treatment of EDC/NHS at the P/DS surface, two representative peaks at 1638 cm^{-1} (amide I) and 1570 cm^{-1} (amide II) were observed in spectrum (iii), which was due to bending vibrations of amide bond formed after the coupling of NHS with carboxybenzyl flanking groups. Similar peaks in the FTIR spectra of EDC/NHS functionalized surface have also been observed previously (Massad-Ivanir et al., 2011). The Anti-ALP immobilized paper surface (P/DS/EDC-NHS/Anti-ALP) was characterized by the presence of two representative bands of protein IR spectrum **(iv)** i.e. amide I and amide II. Multiple peaks present between 1600 and 1700 cm^{-1} band were assigned to the C=O stretching vibrations of amide I. A new sharp peak at 1544 cm^{-1} was clearly observed in the band between 1510 and 1580 cm^{-1} due to the N-H bending vibrations and the C-N stretching vibrations of amide II present in the peptide moieties of Anti-ALP. These stretching vibrations are directly related to the protein (Anti-ALP) backbone conformation, which clearly indicates the immobilization of Anti-ALP onto the paper surface.

Further, in order to validate the sensor-probe fabrication, we have characterized the fabricated probe surface using AFM, where we recorded the surface morphologies after every steps of modification (Fig. 2C) and z-deflection (profile shown in Fig. SI 2) was evaluated as reported earlier (Arun et al., 2016). Firstly, the surface morphology of untreated paper (P) was captured, where the appearance of fibrous topology with z-deflection of 67.38 nm was observed as shown in Fig. 2C (i). Thereafter, we examined the P/DS surface, where we observed granular surface with increased z-deflection (98.20 nm), which is due to the coupling of carboxybenzyl moieties on the paper surface after 4-carboxybenzenediazonium treatment (ii). In the next step, we

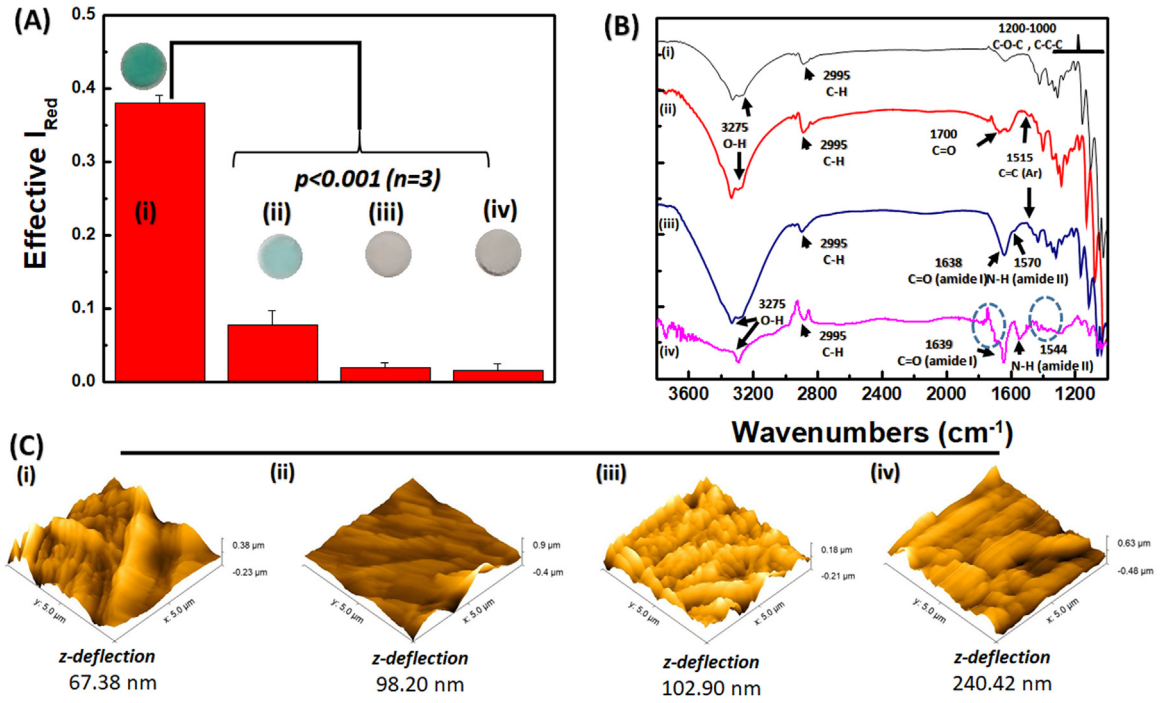

Fig. 2. (A) Histograms showing the comparative Effective I_{Red} of the sensing probe (i) P/DS/EDC-NHS/Anti-ALP/ALP/BCIP; (ii), (iii), and (iv) represents controls; P/DS/ALP/BCIP, P/DS/EDC-NHS/Anti-ALP/ALP, and P/DS/EDC-NHS/Anti-ALP/BCIP, respectively. The respective visuals of paper discs shown above the histogram. (B) FTIR spectra of different stages of the probe fabrication, where (i) P, (ii) P/DS, (iii) P/DS/EDC-NHS, and (iv) P/DS/EDC-NHS/Anti-ALP; (C) AFM micrographs showing the 3D surface topology of (i) P, (ii) P/DS, (iii) P/DS/EDC-NHS, and (iv) P/DS/EDC-NHS/Anti-ALP modified surfaces.

observed the P/DS/EDC-NHS surface, where a clear change in the surface topology was observed with further increase in the z-deflection (102.90 nm) (iii). However, after the immobilization of anti-ALP, the z-deflection increased significantly over two folds (240.42 nm) and a significant change in the surface topology was observed (iv), which was due to the interaction of high molecular weight anti-ALP interacted with the sensor surface. The characterization results obtained from DIC, FTIR and AFM complements each other, indicating the successful fabrication of biosensing probe.

3.3. Analytical performance of P/DS/EDC-NHS/Anti-ALP biosensor

After the successful characterization of the sensor-probe, its analytical performance was evaluated by detecting the ALP in dose dependent manner. For this purpose, at first, the sensor-probe was treated with the buffer without ALP followed by BCIP, where no Effective I_{Red} was obtained. This is because of no colored product formation due to the absence of ALP in the sensing assembly. Thereafter, the P/DS/EDC-NHS/Anti-ALP probe was treated with the different concentrations of ALP followed by the treatment of BCIP and color change was recorded using the smartphone camera. Fig. 3**(A)** displays the Effective I_{Red} responses of the developed biosensor in absence and presence of different concentrations of ALP between 10 and 1000 U/mL. The change in the color of the paper surface clearly shows increase in Effective I_{Red} with increase in the ALP concentrations, indicating that the developed sensor can effectively detect ALP. Based on the Effective I_{Red} responses, two calibration plots were obtained. The linear regression equations for ALP are expressed for low and high concentrations calibration plots are as follow: Effective I_{red}(a.u.) = 0.06549(± 0.00797) + 0.0023(± 0.000183) [ALP] (U/mL) and Effective I_{red}(a.u.) = 0.2930(± 0.0146) + 0.00030(± 0.000028)[ALP](U/mL), with a correlation coefficients of 0.996 and 0.949, respectively. The detection limit of ALP was determined to be 0.870(± 0.07) U/mL (RSD < 5.1%) based on the standard deviation of three repeated measurements of the blank (95.0% confidence level, $n = 3$). The detection ability of the designed biosensor falls well in the range of ALP concentrations present in the raw milk of healthy cow, which was reported to be ~191.0 U/mL (Kitchen, 1981). It is worth mentioning that the overall detection time for ALP in this miniaturized, instrument-less, and commercially-viable method is merely 13.0 min, hence, it could be of tremendous use for onsite analysis

3.4. Selectivity assay

Selectivity is one of the most critical parameter to evaluate the biomedical values of any biosensor (Chandra, 2016; Mahato et al., 2018; Pallela et al., 2016). Thus, we performed selectivity assay using molecules present in milk viz. citric acid, bovine serum albumin (BSA), lactose, casein, vitamin A, vitamin B, and commonly present ions (Ca^{++}, Na^{+}, K^{+}, and Mg^{++}) separately, under the similar experimental conditions. Fig. 3(B) shows a comparative Effective I_{red} for ALP and interfering molecules, where no signals were observed for any of the tested interfering molecules compared to ALP. This was due to the absence of ALP in the sensing matrix, which only generates blue-green precipitate meditated through BCIP. The selectivity of sensor-probe was mathematically analyzed by determining the selectivity coefficient (k_{sel}) using Eq. (3),

$$k_{sel} = \frac{(Signal)_{interferent}}{(Signal)_{ALP}} \quad (3)$$

where k_{sel} is the coefficient of selectivity, $(Signal)_{interferent}$ is the signal strength shown by probe when treated with the interfering molecules, and $(Signal)_{ALP}$ is the signal strength corresponds to the presence of ALP, followed by the treatment of BCIP.

The k_{sel} values for the interfering molecules were found to be extremely low ($k_{sel} \ll 1$), indicating that the fabricated biosensor is highly selective towards ALP. We also performed the T-test and calculated the p-values, which was found to be < *0.001* ($n = 3$) for the interfering molecules, indicating that the selectivity results are statistically significant.

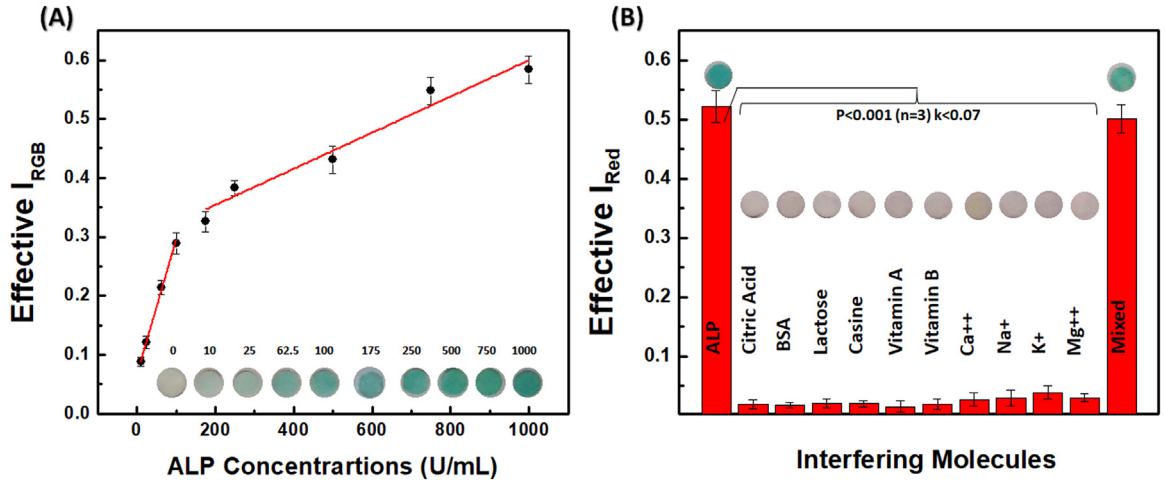

Fig. 3. (A) Calibration plots obtained from the responses of differnt ALP concentration ranging from 10 to 1000 U/mL using the P/DS/EDC-NHS/Anti-ALP probe; (B) Selectivity assay of P/DS/EDC-NHS/Anti-ALP sensor-probe towards interfering molecules and mixed sample analysis.

In real sense, ALP coexists with the interfering molecules in the milk sample, so to make the experimental design more factual, we have performed mixed sample analysis. For this purpose, the ALP was mixed in a solution containing all the interfering molecules in the same concentration found in the milk followed by ALP detection using the developed sensing probe. Interestingly, the sensitivity for ALP detection in this case was found to be 98.6% ($n = 3$) compared when ALP was detected alone, indicating the capability of designed sensor for selective detection of ALP even in a mixed sample solution.

3.5. Real sample analysis

The practical implications of the sensor was evaluated by detecting ALP in milk samples. For this purpose, two different methods were adopted; (i) standard addition and (ii) spike-recovery methods. The intention of standard addition method was to evaluate the unknown concentration of ALP in raw milk samples obtained from villages. For this purpose, ALP was detected in raw milk samples (here no ALP was spiked), using the P/DS/EDC-NHS/Anti-ALP sensor-probe obtained from different locations. Interestingly, in this case, a clear Effective I_{Red} was observed (encircled point of standard addition plot), which increases with the increase in ALP concentrations when spiked from 25 to 100 U/mL. A standard addition plot was obtained which gives a linear regression equation for ALP detection as follows: Effective I_{Red}(a.u.) $= 0.05726(\pm\ 0.00615) + 0.00153(\pm\ 1.59 \times 10^{-4})$[ALP](U/mL) with the correlation coefficient of 0.989. The representative standard addition plot is shown in Fig. 4**A**, where the unknown concentration of the ALP in the raw milk was obtained to be 17.5 ± 1.32 U/mL based on the standard deviation of three repeated measurements (95.0% confidence level, $n = 3$).

Next set of experiments were based on spike-recovery method, which was done to evaluat% recovery of ALP from pasteurized milk samples at various concentrations. In this case, known concentrations of ALP was spiked in the pasteurized milk samples and % recoveries of ALP were calculated using Eq. (4),

$$\%\text{Recovery} = \frac{([A]_{ALP} - [B]_{ALP})}{[C]_{ALP}} \quad (4)$$

where, $[A]_{ALP}$ and $[B]_{ALP}$ are the analytical responses of ALP in the spiked and blank samples, respectively; and $[C]_{ALP}$ is the analytical response of ALP in the standard solutions.

Fig. 4**B** shows a dose depended comparative response of ALP biosensor in milk samples, where increase in the Effective I_{Red} was observed with increase in ALP concentrations, however, no signal was observed when only pasteurized milk samples were analyzed (no ALP added). The sensitivity assay based on % recovery experiment was performed, which shows that the ALP biosensor is able to detect 91.0–100.0% of ALP from the milk samples. The analytical details for recovered ALP concentrations, RSD, and % recovery for all the tested concentrations are represented in Table SI 2 in supplementary-information. The detection limit of ALP in the milk sample was determined to be 1.51 ± 0.17 U/mL (RSD < 11.2%) based on the standard deviation of three repeated measurements of the blank (95.0% confidence level, $n = 3$). Importantly, the ALP concentrations observed in the real sample experiments [(i) and (ii)] falls within the range of ALP levels found in raw milk as reported earlier (Kitchen, 1981; Singh and Ganguli, 1975). These results clearly indicate that the developed sensor-probe can effectively detect ALP in raw and pasteurized milk samples, hence it could be useful to differentiate pasteurized/boiled and raw milk effectively.

3.6. Prototype design and ALP analysis in home kitchen

After getting enthusiastic results in real samples, we extended our work towards the development of a biosensing prototype, which could help in safe, environmental benign storage, and easy handling for in-kitchen analysis. The prototype has been fabricated using a cellulose acetate transparent film (CATF) of dimensions of 20.0 (L) mm × 20.0 mm (W) and 0.25 mm (T), which acts as a supporting layer for the developed paper sensor-probe (P/DS/EDC-NHS/Anti-ALP). The details of the prototype design has been shown in Fig. 5**A**. The modified paper surface (diameter = 5.0 mm) was pasted onto the CATF sheet using glue followed by placing the O-ring of outer diameter of 8.0 mm enclosing the paper disc. This not only provide reservoir for washing/solution exchange, but also provides mechanical strength to the fabricated sensor-probe (P/DS/EDC-NHS/Anti-ALP). In the next step, the upper lid of CATF with hole of 4.0 mm diameter was pasted covering the O-ring. The effective distance between sensor-probe and the upper CATF lid was 1.5 mm, which was sufficient enough for the sample processing. In order to show the applicability of developed prototype ALP detection on kitchen was performed. To do so, ALP containing milk sample was injected through the hole at sensing area of the chip followed by Effective I_{Red} analysis as discussed in earlier section. Interestingly, a blue-green precipitate was observed in the prototype and sensor was able to detect 91.0% of ALP from the originally spiked concentration. Thus, the designed miniaturized ALP sensing kit is extremely powerful for ALP detection and is very handy for the onsite analysis. The real prototype developed has been shown as Fig. 5**B**, which shows before **(i)** and after **(ii)** ALP analysis.

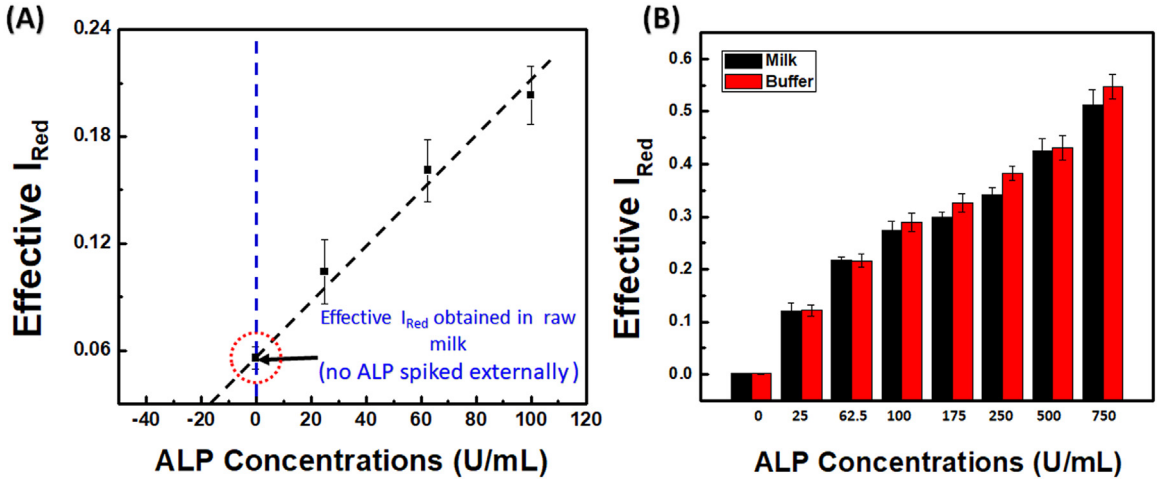

Fig. 4. (A) Standard addition plot obtained for ALP detection in raw milk sample, (B) Comparative dose dependent detection of ALP in pasteurized milk (black bars) and PBS (red bars) based on % recovery (For interpretation of the references to color in this figure legend, the reader is referred to the web version of this article.)

3.7. Storage conditions, stability test, and reproducibility assay

The P/DS/EDC-NHS/Anti-ALP probe was stored at 4 °C after the fabrication in moist condition and the Effective I_{Red} were recorded weekly. We have also studied the shelf-life of the probe, where we tested Effective I_{Red} of P/DS/EDC-NHS/Anti-ALP probe for every third day. The Effective I_{Red} response obtained by the probe shows that the sensor retained the sensitivity of 98.0% up till 14th day, while decrement of the signal was recorded to 88.0 (± 2.15) % till 28th day. The considerably good shelf-life up to four weeks was most likely due to the stable immobilization of anti-ALP and retention of its biological activity on functionalized paper disc. In other words, it is also worth mentioning that the chemical modifications steps performed on the paper disc does not adversely affect the immobilized anti-ALP. After four weeks the signal was dropped up to 84.0%, which was most likely due to the loss of biological activity of anti-ALP and/or the degradation of the chemical modification steps. The reproducibility of the biosensor was evaluated, which showed the RSD < 4.7% ($n = 3$) and disc to disc RSD was < 5.2% even when the same fabrication process was followed. This minor variation was most likely due to the negligible variation in the sensor fabrication process and handling error.

4. Conclusions

The present study describes the development of dot-spot, economical, paper-based biosensor for ALP detection in milk based on DIC integrated with smartphone. The fabrication of sensor-probe was characterized by DIC, FTIR, and AFM. The selection of color channel for

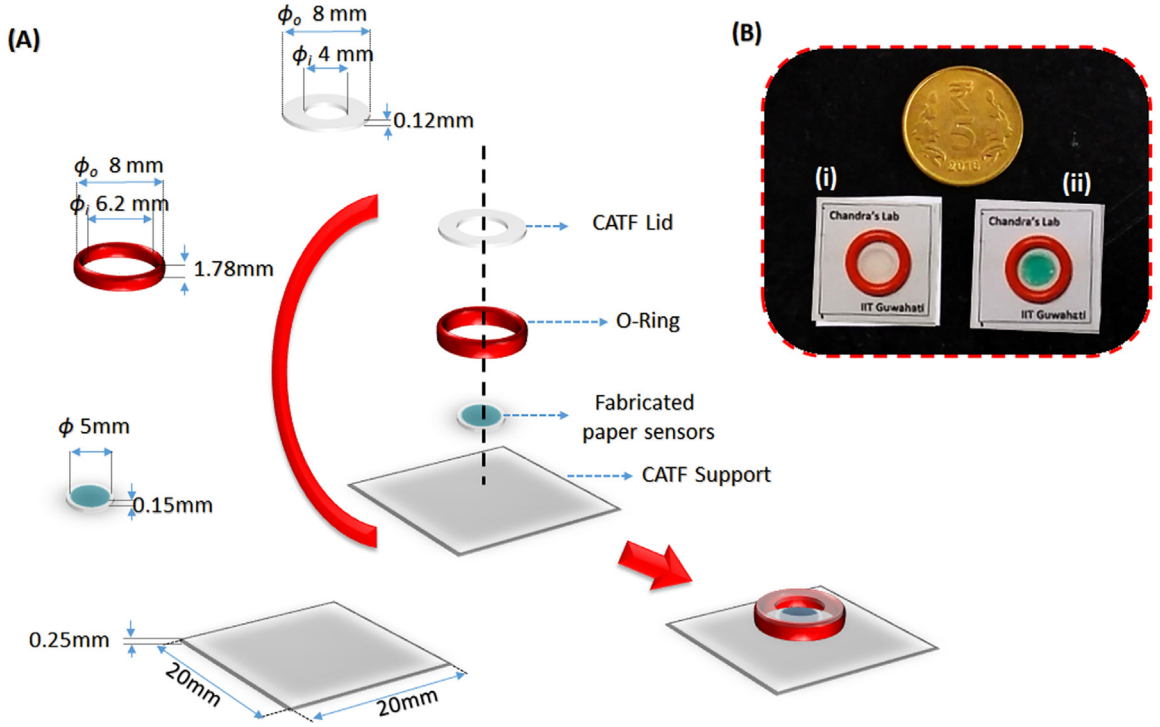

Fig. 5. (A) A detailed description of designed prototype with dimensions and (B) the actual prototype showing the color change in the (i) before and (ii) after interaction of ALP with the P/DS/EDC-NHS/Anti-ALP sensor-probe (For interpretation of the references to color in this figure legend, the reader is referred to the web version of this article.)

colorimetric analyses was demonstrated for the first time in a paper matrix to the best of our knowledge, where the maximum sensitivity was observed for red channel. The limit of detection of proposed biosensor is 0.870 (± 0.07) U/mL, which is suitable for discriminating the raw milk (contains ~191.0 U/mL ALP) from the pasteurized/boiled milk at point of collection in merely 13.0 min without using any additional instrument. The biosensor was found to be highly selective (k_{sel}« *1*; $p < 0.001$; $n = 3$) towards ALP and shows 91–100% recoveries of ALP from raw milk samples. Based on the sensing principle, a miniaturized kit has been developed and demonstrated for ALP detection in kitchens, indicating is real household and prospective industrial potential. In future, the sensing platform/principle described herein can be extended towards the detection of various molecules in different matrices.

Acknowledgement

Authors acknowledge Ramanujan Fellowship (SB/S2/RJN-042/2015) awarded to Dr. Pranjal Chandra by the Department of Science and Technology – Government of India. KM acknowledges Ph.D. research fellowship supported by Indian Institute of Technology - Guwahati (IIT-G). Authors thanks Center for Nanotechnology, IIT-G for AFM analysis.

Appendix A. Supporting information

Supplementary data associated with this article can be found in the online version at doi:10.1016/j.bios.2018.12.006.

References

Akhtar, M.H., Hussain, K.K., Gurudatt, N.G., Chandra, P., Shim, Y.-B., 2018. Biosens. Bioelectron. 116, 108–115.
Al-Qadiri, H., Lin, M., Al-Holy, M., Cavinato, A., Rasco, B.A., 2008. J. Dairy Sci. 91 (3), 950–958.
Arun, R.K., Singh, P., Biswas, G., Chanda, N., Chakraborty, S., 2016. Lab Chip 16 (18), 3589–3596.
Babaei, H., Mansouri-Najand, L., Molaei, M.M., Kheradmand, A., Sharifan, M., 2007. Vet. Res. Commun. 31 (4), 419–425.
Barkworth, H., Hosking, Z., 1952. Proc. Soc. Appl. Bacteriol. 15 (1), 116–125.
Chandan, R.C., Kilara, A., Shah, N.P., 2015. Dairy Processing and Quality Assurance, 2nd ed. Wiley-Blackwell.
Chandra, P., 2016. Nanobiosensors for Personalized and Onsite Biomedical Diagnosis. The Institution of Engineering and Technology, London.
Chandra, P., Koh, W.C.A., Noh, H.-B., Shim, Y.-B., 2012. Biosens. Bioelectron. 32 (1), 278–282.
Chen, C.-C., Tai, Y.-C., Shen, S.-C., Tu, Y.-Y., Wu, M.-C., Chang, H.-M., 2006. Food Chem. 95 (2), 213–220.
Choodum, A., Keson, J., Kanatharana, P., Limsakul, W., Wongniramaikul, W., 2017. Sens. Actuators B: Chem. 252, 463–469.
Fasken, J.E., McClure, A.D., 1940. Can. J. Comp. Med. Vet. Sci. 4 (5), 128–137.
Firdaus, M.L., Alwi, W., Trinoveldi, F., Rahayu, I., Rahmidar, L., Warsito, K., 2014. Procedia Environ. Sci. 20, 298–304.
Gaucheron, F., 2011. J. Am. Coll. Nutr. 30 (sup5), 400S–409S.
Hosseini, S., Vázquez-Villegas, P., Martínez-Chapa, S.O., 2017. Appl. Sci. 7 (8), 863.
Ito, S., Yamazaki, S.-I., Kano, K., Ikeda, T., 2000. Anal. Chim. Acta 424 (1), 57–63.
Jay-Russell, M.T., 2010. Clin. Infect. Dis. 51 (12), 1418–1419.
Kitchen, B.J., 1981. J. Dairy Res. 48 (1), 167–188.
Kulmyrzaev, A.A., Levieux, D., Dufour, É., 2005. J. Agric. Food Chem. 53 (3), 502–507.
Lin, B., Yu, Y., Cao, Y., Guo, M., Zhu, D., Dai, J., Zheng, M., 2018. Biosens. Bioelectron. 100, 482–489.
Mahato, K., Maurya, P.K., Chandra, P., 2018. 3 Biotech 8 (3), 149.
Mahato, K., Srivastava, A., Chandra, P., 2017. Biosens. Bioelectron. 96, 246–259.
Massad-Ivanir, N., Shtenberg, G., Tzur, A., Krepker, M.A., Segal, E., 2011. Anal. Chem. 83 (9), 3282–3289.
Nayak, N., 2018. Res. Rev.: J. Dairy Sci. Technol. 6 (3), 17–29.
Pallela, R., Chandra, P., Noh, H.-B., Shim, Y.-B., 2016. Biosens. Bioelectron. 85, 883–890.
Park, L., Bae, H., Kim, Y.-T., Lee, J.H., 2011. Anal. Methods 3 (1), 156–160.
Parkin, A., 2016. Viewing 8-bit Image. Digital Imaging Primer. Springer, pp. 643–645.
Payne, C., Wilbey, R.A., 2009. Int. J. Dairy Technol. 62 (3), 308–314.
Peng, B., Chen, G., Li, K., Zhou, M., Zhang, J., Zhao, S., 2017. Food Chem. 230, 667–672.
Rankin, S.A., Christiansen, A., Lee, W., Banavara, D.S., Lopez-Hernandez, A., 2010. J. Dairy Sci. 93 (12), 5538–5551.
Rateni, G., Dario, P., Cavallo, F., 2017. Sensors 17 (6), 1453.
Rola, J.G., Sosnowski, M., 2010. Bull. Vet. Inst. Pulawy 54, 537–542.
Rozenberg, S., Body, J.-J., Bruyère, O., Bergmann, P., Brandi, M.L., Cooper, C., Devogelaer, J.-P., Gielen, E., Goemaere, S., Kaufman, J.-M., Rizzoli, R., Reginster, J.-Y., 2016. Calcif. Tissue Int. 98 (1), 1–17.
Scharer, H., 1938. J. Dairy Sci. 21 (1), 21–34.
Serra, B., Morales, M.D., Reviejo, A.J., Hall, E.H., Pingarrón, J.M., 2005. Anal. Biochem. 336 (2), 289–294.
Singh, L.N., Ganguli, N.C., 1975. Indian J. Dairy Sci. 28, 67–68.
Soares, C., Fonseca, L., Leite, M., Oliveira, M., 2013. Arq. Bras. Med. Vet. Zootec. 65 (4), 1223–1230.
Tajima, N., Takai, M., Ishihara, K., 2011. Anal. Chem. 83 (6), 1969–1976.
Trilling, A.K., Beekwilder, J., Zuilhof, H., 2013. Analyst 138 (6), 1619–1627.
Yalcin, B.K., Atasever, S., 2018. Turk. J. Agric. Food Sci. Technol. 6 (5), 557–560.
Yetisen, A.K., Akram, M.S., Lowe, C.R., 2013. Lab Chip 13 (12), 2210–2251.
Yu, L., Shi, Z., Fang, C., Zhang, Y., Liu, Y., Li, C., 2015. Biosens. Bioelectron. 69, 307–315.